separations

MDPI

Article

Hydrophobically Modified Anionic Polyacrylamide for Flocculation–Dewatering of Low-Rank Ultrafine Flotation Clean Coal

Qiming Zhuo [1], Rong Zou [1], Xuan Du [1], Leilei Gao [2], Hongxiang Xu [1], Jiushuai Deng [1], Wenli Liu [1], He Zhang [3,*] and Kejia Ning [4,*]

[1] School of Chemical and Environmental Engineering, China University of Mining & Technology (Beijing), Beijing 100083, China
[2] Datang Tongzhou Technology Co., Ltd., Beijing 100040, China
[3] School of Mining Engineering, Heilongjiang University of Science and Technology, Harbin 101601, China
[4] National Geological Library of China (Geoscience Documentation Center), China Geological Survey, Beijing 100083, China
* Correspondence: zhe9127@163.com (H.Z.); ningkejia@foxmail.com (K.N.); Tel.: +86-13161290415 (H.Z.)

Abstract

Low-rank ultrafine flotation clean coal typically yields filter cake moisture above 20% due to abundant oxygen-containing functional groups and strong surface hydrophilicity. Conventional polyacrylamide (PAM) flocculants are hydrophilic and improve dewatering only by altering cake porosity, not by reducing particle surface hydrophilicity, so they remove little adsorbed water. In this study, hydrophobically modified anionic polyacrylamides (HMAPAM) were synthesized by grafting lauryl acrylate onto APAM. FTIR, ^{1}H NMR, XPS, and SEM confirmed the grafting and progressive enrichment of hydrophobic alkyl chains on the surface. Moderate hydrophobic modification markedly improved solid–liquid separation. HMAPAM-D (APAM/LA = 4.5:0.5) achieved a settling velocity of 0.817 cm/s at 9 mg/L, 50.2% higher than APAM, and reduced filter cake moisture to 16.64% at 1 mg/L under 0.6 MPa versus 19.39% for unmodified APAM. Excessive modification (HMAPAM-E, 4:1) promoted intramolecular self-association, producing heterogeneous flocs and higher filtration resistance that degraded dewatering efficiency. The performance gain stems from hydrophobic association combined with adsorption bridging. These results clarify how hydrophobic group content controls flocculation and dewatering, informing the design of better flocculants for this type of coal slurry.

Keywords: hydrophobic modification; low-rank coal; flocculation–dewatering; filter cake moisture; hydrophobic association

Check for updates

Received: 29 April 2026
Revised: 8 June 2026
Accepted: 10 June 2026
Published: 12 June 2026

Copyright: © 2026 by the authors. Licensee MDPI, Basel, Switzerland. This article is an open access article distributed under the terms and conditions of the Creative Commons Attribution (CC BY) license.

1. Introduction

Froth flotation serves as the principal method for recovering fine coal slimes, though subsequent dewatering is required to render the clean coal product suitable for storage, transportation, and utilization [1,2]. With the continuous advancement of coal mining mechanization, the proportion of ultrafine particles in raw coal feed has progressively increased, particularly for particles smaller than 0.5 mm and slime fractions below 0.045 mm [3,4]. Low-rank coals exhibit a well-developed pore structure and abundant oxygen-containing functional groups, which confer strong surface hydrophilicity; consequently, dewatering of their flotation clean coal products presents particular difficulties [5,6]. Pressure filtration,

as the predominant mechanical dewatering technique, typically yields filter cake moisture contents exceeding 20% when processing low-rank ultrafine flotation clean coal. Excessive moisture in the clean coal product directly diminishes calorific value, elevates transportation costs, and causes winter freezing; in coking applications, it prolongs carbonization time and reduces coke yield [7,8].

Mechanical dewatering and process parameter optimization constitute the principal industrial strategies for mitigating the aforementioned challenges [9,10]. Modifying operating variables such as feed solids concentration, filtration pressure, and pressure holding time can reduce filter cake moisture within a limited range; however, these variables are subject to mutual constraints, yielding a narrow optimal operating window [11,12]. Introducing coarse particles into fine clean coal to construct a high-porosity skeleton structure enhances filter cake permeability, yet precise control of the blending ratio remains difficult, and the attendant risk of elevated product ash content poses a significant concern [13]. Membrane filter presses enable additional removal of capillary water through secondary squeezing, while ultra-high pressure filtration systems can reduce coal slime moisture to 14–17% [14,15]. Nevertheless, such technologies entail substantial capital investment, and the improvement in dewatering efficiency for ultrafine materials is approaching its upper limit [16,17].

Chemical conditioning represents the most economically viable strategy for enhancing the dewatering of ultrafine coal slimes, with polyacrylamide (PAM) and its derivatives being the most widely employed [18,19]. PAM molecules facilitate the aggregation of fine particles into larger flocs through charge neutralization and adsorption bridging [20,21]. The resultant flocculated filter cake possesses higher porosity than the dense structure formed by dispersed particles, thereby enhancing filter cake permeability [22,23]. Cationic polyacrylamide (CPAM) typically exhibits superior dewatering performance relative to other ionic types, attributable to the strong electrostatic attraction between its positively charged functional groups and the negatively charged coal surfaces [24,25]. Nevertheless, the limitations of conventional PAM in low-rank coal dewatering are pronounced: its molecular chains are inherently hydrophilic, which compromises flocculation efficacy on the strongly hydrophilic surfaces characteristic of low-rank coals; the optimal dosage window is narrow, as insufficient addition leads to incomplete flocculation, whereas excess dosage induces floc restabilization or filter cloth blinding; and the flocculation performance is highly sensitive to water chemistry conditions [26]. Fundamentally, PAM promotes dewatering solely by modifying the macroscopic pore structure of the filter cake without reducing the surface hydrophilicity of coal particles, thereby offering limited effectiveness in removing adsorbed water [27,28].

Previous studies have demonstrated that hydrophobically modified polyacrylamide flocculants can effectively improve the aggregation and dewatering behavior of fine coal slurries [29]. For example, Guo et al. reported that amphiphilic PAM systems containing hydrophobic side chains enhanced floc growth and reduced filter cake moisture through hydrophobic association effects [30]. Yang et al. further showed that moderate hydrophobic modification promoted adsorption bridging and improved filtration performance, whereas excessive hydrophobic content could induce polymer self-association and deteriorate floc structure stability [31]. Although these studies confirmed the potential of hydrophobic modification for coal slurry dewatering, the relationship between hydrophobic modification degree, polymer chain accessibility, and flocculation dewatering behavior remains insufficiently understood, particularly for low-rank coal slurries rich in oxygen-containing functional groups.

Motivated by these considerations, low-rank long-flame coal flotation clean coal collected from a coal preparation plant in Yulin, Shaanxi Province, was selected as the

research object in this study. Although hydrophobically modified polyacrylamide flocculants have been reported previously, the relationship between hydrophobic modification degree, polymer chain conformation, floc structure evolution, and coupled flocculation–dewatering behavior remains insufficiently understood, particularly for low-rank ultrafine coal slurry systems containing abundant oxygen-containing functional groups. To address this issue, a series of hydrophobically modified anionic polyacrylamides (HMAPAMs) was synthesized through free-radical graft copolymerization using anionic polyacrylamide (APAM) as the backbone and lauryl acrylate (LA) as the hydrophobic monomer. It was hypothesized that moderate hydrophobic modification could enhance adsorption affinity toward coal particles and promote the formation of permeable floc networks through intermolecular hydrophobic association, whereas excessive hydrophobic group incorporation might induce intramolecular self-association and chain collapse, thereby reducing effective bridging efficiency.

The effects of hydrophobic modification degree on flocculation–sedimentation and pressure filtration dewatering behaviors were systematically investigated. The chemical structure and microstructural characteristics of the synthesized flocculants were analyzed using Fourier transform infrared spectroscopy (FTIR) (Thermo Fisher Scientific, Waltham, MA, USA), proton nuclear magnetic resonance (^{1}H NMR) (Bruker BioSpin, Rheinstetten, Germany), X-ray photoelectron spectroscopy (XPS) (Thermo Fisher Scientific, East Grinstead, UK), and scanning electron microscopy (SEM) (Thermo Fisher Scientific, Brno, Czech Republic). Combined with settling and pressure filtration experiments, the evolution characteristics of floc structure and their influence on dewatering performance were further elucidated. This study aims to establish the relationship between hydrophobic group content, polymer association behavior, floc structure evolution, and dewatering performance, thereby providing theoretical guidance for the molecular design of efficient dewatering flocculants for low-rank coal slurry systems.

2. Experimental

2.1. Properties of Coal Sample

The coal sample was collected from the flotation concentrate of a coal preparation plant in Yulin, Shaanxi Province, China. The particle size distribution and proximate analysis of the coal sample were determined according to the Chinese national standards GB/T 477–2008 (particle size analysis of coal) [32] and GB/T 212–2008 (proximate analysis of coal) [33], respectively. The contents of C, H, O, N, and S were measured using an Elementar UNICUBE elemental analyzer (Elementar Analysensysteme GmbH, Langenselbold, Germany).

The −0.045 mm fraction accounts for 54.70% of the sample by mass (Table 1); such a fine particle size distribution complicates slurry sedimentation and dewatering.

Table 1. Particle size distribution of coal sample.

Size Fraction/mm	Yield/%	Ash Content/%
0.5–0.25	4.63	4.30
0.25–0.125	13.69	3.85
0.125–0.074	15.41	3.43
0.074–0.045	11.58	3.66
<0.045	54.70	4.35
Total	100.00	4.06

The physicochemical properties of the coal sample are summarized in Table 2. Proximate analysis showed that the coal sample possessed an ash yield (Aad, air-dried basis) of

4.16% and a volatile matter yield (Vad, air-dried basis) of 31.33%. Ultimate analysis indicated that the contents of carbon (Cdaf, dry ash-free basis), hydrogen (Hdaf, dry ash-free basis), and oxygen (Odaf, dry ash-free basis) were 74.64%, 4.65%, and 18.51%, respectively. The relatively high oxygen content suggests the presence of abundant oxygen-containing functional groups on the coal surface. These characteristics are typical of low-rank coal, which possesses both hydrophilic oxygen-containing groups and hydrophobic aromatic–aliphatic structures.

Table 2. Proximate and ultimate analyses of coal sample.

Proximate Analysis				Ultimate Analysis				
M_{ad}	A_{ad}	V_{ad}	FC_{ad}	C_{daf}	H_{daf}	O_{daf}	N_{daf}	S_{daf}
4.97	4.16	31.33	59.54	74.64	4.65	18.51	0.95	1.25

FTIR spectrum of the coal sample (Figure 1) reveals a surface bearing both hydrophilic oxygenated groups and hydrophobic aliphatic–aromatic structures. The broad band at ~3415 cm^{-1} corresponds to O–H stretching of hydrogen-bonded, phenolic, and alcoholic hydroxyls, together with adsorbed water. The band at 1033 cm^{-1} reflects C–O and Si–O stretching, indicating oxygen-containing functionalities and aluminosilicate minerals. Peaks at 2920 and 2855 cm^{-1} are assigned to asymmetric and symmetric C–H stretching of aliphatic $–CH_2–$ groups. Bands at 1595 cm^{-1} and 1434 cm^{-1} are ascribed to aromatic C=C stretching and CH_2 scissoring (or aromatic ring vibration), respectively. These polar hydroxyls provide hydrogen-bonding sites for flocculant adsorption. FTIR reveals a coal surface with a hydrophobic aromatic backbone bearing oxygenated polar groups. Such surface heterogeneity allows HMAPAM to bind coal particles through hydrophobic association and hydrogen bonding, promoting interparticle bridging.

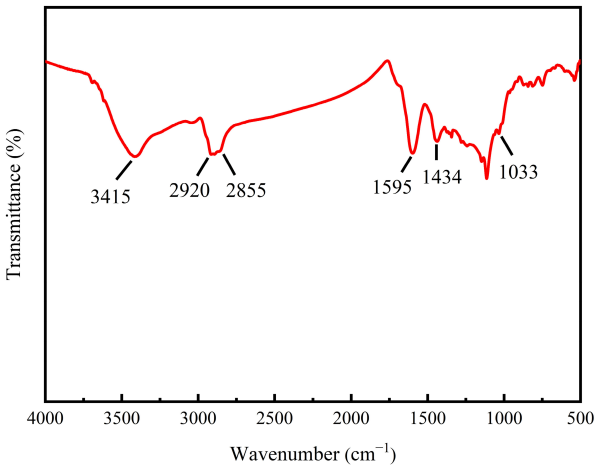


Figure 1. FTIR spectrum of coal sample.

2.2. Materials

Commercial anionic polyacrylamide (APAM, Mw = 1.2 × 10^7 g/mol, hydrolysis degree: 20–30%) was used as the hydrophilic polymer backbone, while lauryl acrylate (LA) served as the hydrophobic grafting monomer. The APAM sample was supplied by Shanghai Dibo Biotechnology Co., Ltd. (Shanghai, China). Free-radical graft copolymerization was initiated using a redox initiator system consisting of sodium persulfate ($Na_2S_2O_8$) and sodium bisulfite ($NaHSO_3$), with Tween-80 employed as the emulsifier to facilitate dispersion of the hydrophobic monomer in the aqueous phase. All reagents used in this study were of analytical grade.

2.3. Experimental Methods

The experimental workflow is illustrated in Figure 2, comprising (i) HMAPAM synthesis and characterization at varied monomer feed ratios, (ii) flocculation–dewatering evaluation through settling and pressure filtration tests, and (iii) microscale mechanism analysis.

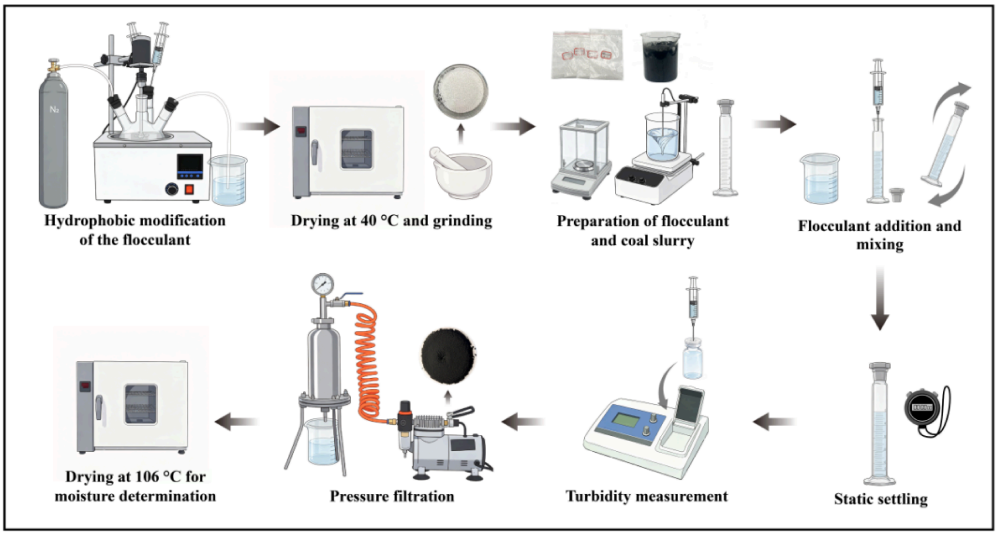


Figure 2. Schematic illustration of the experimental workflow.

2.3.1. Preparation of Hydrophobically Modified APAM

HMAPAM was synthesized by free-radical graft copolymerization of LA onto APAM in a surfactant-assisted aqueous graft copolymerization system. The hydrophobic lauryl groups were introduced as pendant side chains onto the APAM backbone through free-radical graft copolymerization. Samples HMAPAM-A to HMAPAM-E were prepared at APAM/LA mass ratios of 4.8:0.2, 4.7:0.3, 4.6:0.4, 4.5:0.5, and 4:1. Total monomer loading was 5 g per 500 g aqueous phase. Tween-80 was added at 30 wt% of LA. The redox initiator ($Na_2S_2O_8$/$NaHSO_3$, 1:1.3 by mass) was used at 0.3 wt% of total monomer (0.0065 g $Na_2S_2O_8$ and 0.0085 g $NaHSO_3$ per batch).

APAM was dissolved in deionized water with magnetic stirring. LA and Tween-80 were emulsified at 80 °C and added dropwise to the APAM solution at 40 °C under continuous stirring. The pH was adjusted to 7.0 with 0.1 mol/L NaOH and HCl. The mixture was purged with nitrogen under stirring for 30 min for deoxygenation; sodium persulfate was then introduced to initiate polymerization. After 30 min, sodium bisulfite solution was added dropwise over 30 min. Polymerization proceeded at 40 °C under nitrogen for 2 h. The product was precipitated by adding three volumes of anhydrous ethanol. The supernatant was decanted, and the precipitate was washed two to three times with fresh ethanol, dried at 40 °C for 24 h, and ground to yield HMAPAM as a dry powder.

2.3.2. FTIR Characterization

FTIR analysis was conducted to identify functional group variations associated with hydrophobic modification of APAM.FTIR spectra of APAM and HMAPAM were recorded on a Nicolet 6700 spectrometer (Thermo Fisher Scientific, Waltham, MA, USA) over 4000–400 cm^{-1} at 4 cm^{-1} resolution (32 scans). Samples were dried at 40 °C prior to analysis and ground with spectroscopic-grade KBr into thin pellets.

2.3.3. ^{1}H NMR Characterization

^{1}H NMR analysis was employed to characterize the chemical environment of proton groups and confirm the introduction of hydrophobic alkyl chains into the polymer structure.

^{1}H NMR spectra of APAM and HMAPAM were recorded on a Bruker AVANCE III 400 MHz spectrometer (16 scans) (Bruker BioSpin, Rheinstetten, Germany). Samples were dissolved in D_2O and transferred to NMR tubes.

2.3.4. XPS Characterization

XPS analysis was performed to investigate surface elemental composition and chemical bonding states of the synthesized flocculants. XPS spectra of APAM and HMAPAM were recorded on a Thermo Scientific K-Alpha spectrometer (Thermo Fisher Scientific, East Grinstead, UK) (monochromatic Al Kα, hv = 1486.6 eV; pass energy 30.0 eV; step size 1.0 eV). Samples were dried at 40 °C, ground, and pressed into pellets. Spectra were charge-corrected to C 1s at 284.8 eV, and high-resolution peaks were deconvoluted.

2.3.5. SEM Characterization

SEM (Thermo Fisher Scientific, Brno, Czech Republic) observations were primarily used for qualitative analysis of floc morphology and surface microstructure. SEM images of APAM, HMAPAM, and flocculated coal samples were obtained on a Regulus 8100. Samples were dried at 40 °C, mounted on aluminium stubs with conductive tape, and sputter-coated with gold.

2.3.6. Coal Slurry Settling Tests

A coal slurry of 40 g/L was prepared by dispersing 20 g of coal sample in 500 mL of water. The suspension was agitated on a magnetic stirrer for 1 min and transferred into a 500 mL sedimentation cylinder. A graduated glass cylinder with an inner diameter of 56 mm and a height of 410 mm was used. The cylinder was sealed and inverted 20 times to ensure uniform dispersion. A flocculant solution was added onto the liquid surface with a syringe; the cylinder was stoppered, inverted 12 times, and placed vertically to start settling. The interface migration behavior between the 450 mL and 250 mL graduations was monitored and used to evaluate settling performance. After 20 min, supernatant turbidity was measured, and compression layer height was recorded. The supernatant was withdrawn with a syringe and transferred to a turbidimeter cuvette. Dosages of 1–9 mg/L were tested for each flocculant, with at least three replicates at each level.

2.3.7. Pressure Filtration Dewatering Tests

Pressure filtration was conducted with a polypropylene membrane. Pressure filtration was performed at a constant filtration pressure of 0.6 MPa using a polypropylene membrane with a diameter of 10 cm. The slurry preconditioned by 20 min sedimentation was charged into the filter cylinder and pressurized with compressed air. Cake formation time was recorded from valve opening to complete filtrate discharge; filtrate turbidity was measured. The cake was retrieved and homogenized; a portion (approx. 1 g) was dried at 105 °C for 2 h to determine moisture content.

3. Results and Discussion

3.1. Structural Characterization of APAM and HMAPAM

3.1.1. FTIR Analysis

FTIR spectra of APAM and HMAPAM (A–E) are presented in Figure 3. The broad absorption band observed at 3200–3500 cm^{-1}, corresponding to N–H and O–H stretching vibrations, was retained in all samples, indicating that the amide-based hydrophilic backbone structure of APAM remained preserved after hydrophobic modification. In contrast, the absorption bands at 2850–2950 cm^{-1} assigned to aliphatic C–H stretching vibrations, together with the characteristic C–O–C stretching band at 1000–1200 cm^{-1}, gradually in-

tensified from HMAPAM-A to HMAPAM-E with increasing LA dosage. These changes confirm the successful introduction of hydrophobic lauryl side chains onto the APAM backbone through graft copolymerization.

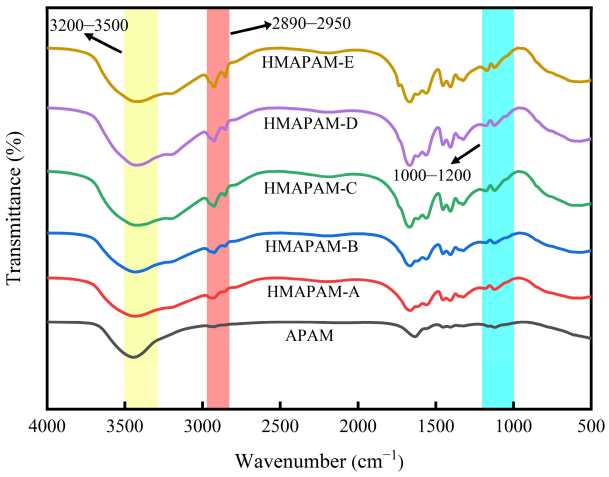


Figure 3. FTIR spectra of pristine APAM and HMAPAM (A–E).

The progressive enhancement of hydrophobic alkyl-related functional groups suggests that the hydrophobic association capability of the polymer chains was strengthened with increasing LA content. Moderate incorporation of hydrophobic side chains is expected to enhance intermolecular hydrophobic interactions, thereby promoting polymer chain extension and adsorption bridging between coal particles. However, excessive hydrophobic group incorporation may increase intramolecular self-association tendencies, resulting in partial chain curling and reduced steric accessibility of active adsorption sites. This structural evolution is consistent with the subsequently observed variations in flocculation and dewatering performance.

3.1.2. ^{1}H NMR Analysis

^{1}H NMR spectra of APAM and HMAPAM (A–E) are shown in Figure 4. APAM exhibited characteristic proton signals at δ 1.5–2.5 ppm, corresponding to the backbone –CH_2– and –CH– groups, while no obvious resonance signals were observed in the long-chain alkyl region. After hydrophobic modification, new characteristic peaks appeared at δ ≈ 0.8–1.0 ppm (terminal –CH_3), δ ≈ 1.2–1.8 ppm (methylene groups in long alkyl chains), and δ ≈ 2.0–2.5 ppm (–CH_2– adjacent to ester groups), confirming the successful incorporation of lauryl side chains into the APAM backbone. The gradual increase in the intensity of these alkyl-related peaks from HMAPAM-A to HMAPAM-E further indicates the progressive enhancement of hydrophobic group content with increasing LA dosage.

Notably, the alkyl-chain-related resonance peaks became significantly broadened in HMAPAM-E. This phenomenon suggests restricted segmental mobility of the polymer chains caused by excessive hydrophobic association. Moderate hydrophobic modification is conducive to intermolecular association and extension of polymer chains in solution, which favors adsorption bridging and floc network formation. However, excessive hydrophobic group incorporation may promote intramolecular self-association and partial chain collapse, thereby reducing effective chain extension and steric accessibility for particle capture. These conformational changes are considered closely related to the subsequently observed deterioration in settling and filtration performance at excessive LA dosage.

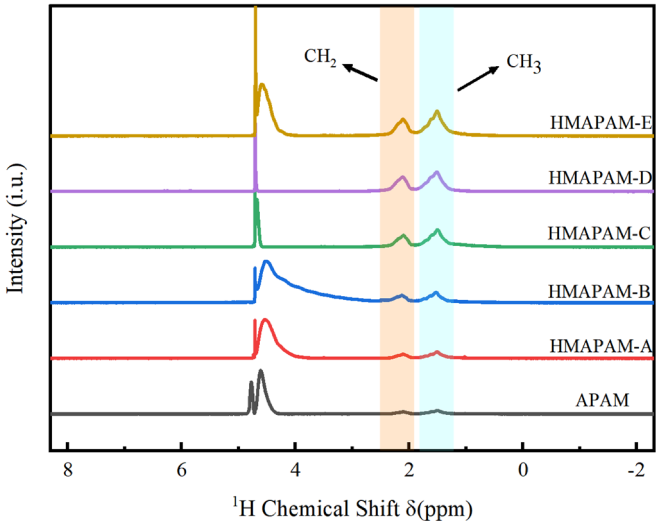


Figure 4. ^{1}H NMR spectra of pristine APAM and HMAPAM (A–E).

3.1.3. XPS Analysis

XPS survey spectra (Thermo Fisher Scientific, East Grinstead, UK) of APAM and HMAPAM are presented in Figure 5. All samples exhibited similar elemental compositions dominated by C and O, accompanied by minor amounts of N and Na. Compared with APAM, the HMAPAM samples displayed progressively enhanced C 1s signals and weakened O 1s signals with increasing LA dosage, indicating gradual enrichment of hydrophobic carbon-containing groups on the polymer surface.

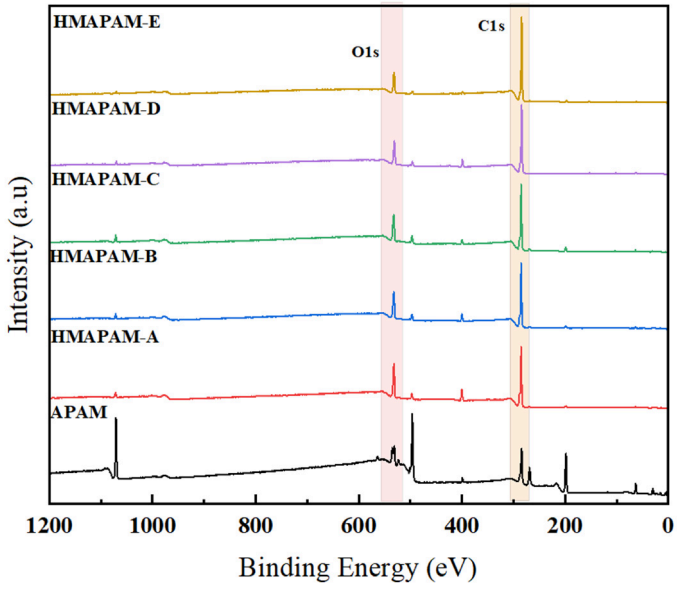


Figure 5. XPS survey spectra of pristine APAM and HMAPAM (A–E).

Quantitative analysis further confirmed this trend. The atomic fraction of carbon increased from 67.36% for APAM to 72.98–85.57% for HMAPAM-A to HMAPAM-E, whereas the oxygen content decreased correspondingly from 26.85% to 19.11–12.49%. The increase in surface carbon content, together with the reduction in oxygen-containing groups, demonstrates the successful incorporation of hydrophobic lauryl side chains through graft copolymerization. More importantly, these compositional variations suggest a gradual reduction in surface polarity and hydrophilicity of the polymer chains with increasing LA content.

Moderate hydrophobic modification is expected to enhance the adsorption affinity between the polymer and partially hydrophobic regions on the coal surface, thereby improving interparticle bridging and floc formation. Simultaneously, partial shielding of oxygen-containing functional groups may weaken hydration interactions and reduce adsorbed water retention within the filter cake. However, excessive hydrophobic modification may intensify hydrophobic self-association among polymer chains, leading to reduced chain extension and deterioration of effective bridging performance. To further elucidate the changes in functional group chemistry, high-resolution C 1s and O 1s spectra were subsequently analyzed.

High-resolution C 1s spectra are presented in Figure 6. Deconvolution results indicate that the relative proportion of nonpolar C–C/C–H groups increased progressively from 76.82% for APAM to 82.65% for HMAPAM-E with increasing LA dosage. In contrast, the proportion of polar carbonyl groups (C=O) decreased markedly from 11.71% to 2.40%, whereas other oxygen-containing carbon species remained relatively unchanged. These results demonstrate a gradual transition of the polymer surface chemistry from a relatively polar state to a more hydrophobic carbon-dominated surface following LA incorporation.

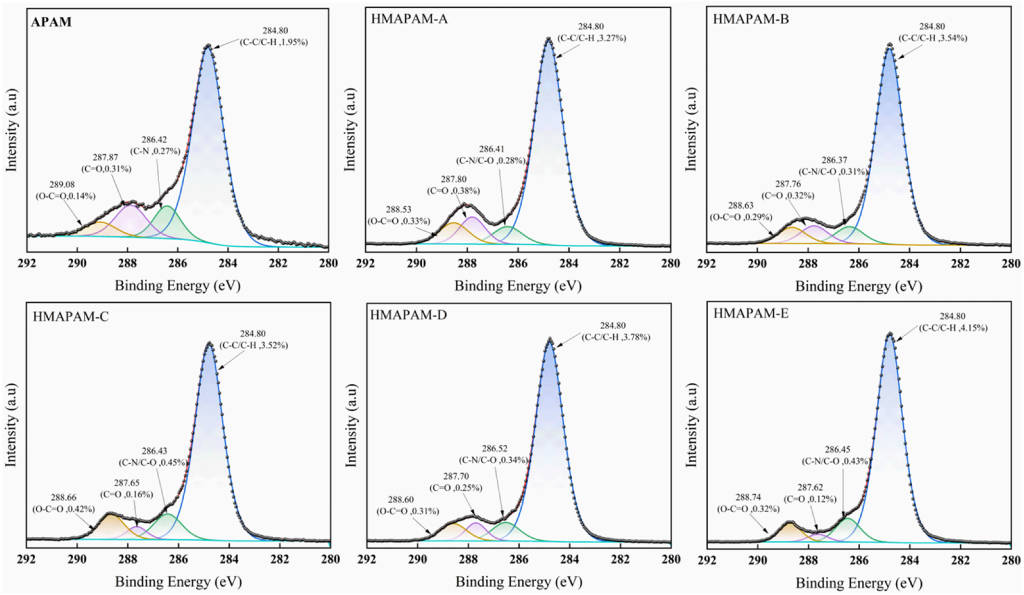


Figure 6. High-resolution C 1s XPS spectra of pristine APAM and HMAPAM (A–E).

The enrichment of nonpolar alkyl carbon species is expected to enhance hydrophobic interactions between the polymer chains and hydrophobic domains on the coal surface, thereby improving adsorption affinity and interparticle bridging during flocculation. Meanwhile, the reduction in polar oxygen-containing groups may weaken hydrogen-bonding interactions with water molecules, which is beneficial for reducing bound water retention within the filter cake. However, excessive enrichment of hydrophobic carbon groups may also strengthen polymer self-association in solution, potentially restricting chain extension and decreasing effective bridging accessibility at high LA dosage.

High-resolution O 1s spectra are presented in Figure 7. Compared with APAM, the distribution of oxygen-containing functional groups in HMAPAM changed significantly after hydrophobic modification. In APAM, C–O species constituted the predominant oxygen-containing structure. With increasing LA incorporation, the relative proportion of oxygen-containing functional groups exhibited a redistribution behavior. At relatively low LA dosage, the contents of several oxygenated structures increased slightly, which may be associated with the introduction of ester-containing side chains during graft copolymerization. However, at higher LA ratios, the proportion of carbonyl groups (C=O) decreased

markedly from 37.49% to 8.49%, while the –COO– content reached a maximum at the APAM/LA ratio of 4:1. The C–O component increased initially and then decreased slightly at excessive LA dosage.

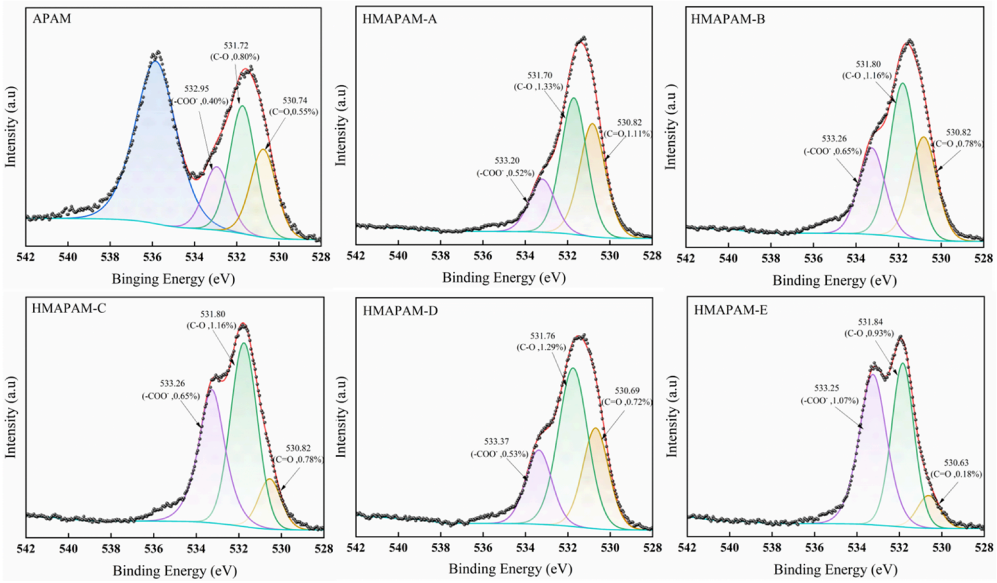


Figure 7. High-resolution O 1s XPS spectra of pristine APAM and HMAPAM (A–E).

Although oxygen-containing groups were still present in the modified polymers, their surface exposure appeared to be partially shielded by the grafted hydrophobic alkyl chains. This shielding effect suggests a reduction in the effective exposure of hydrophilic functional groups to water molecules, thereby weakening hydration interactions and reducing the retention tendency of adsorbed water within the floc structure and filter cake. Moderate hydrophobic shielding may therefore contribute to improved dewatering performance by balancing hydrophobic association and polymer chain accessibility. In contrast, excessive hydrophobic modification may intensify polymer self-association and reduce effective interaction between the polymer and coal particles, which is unfavorable for maintaining an extended and permeable floc network.

3.1.4. SEM Analysis

SEM was used to examine the morphological evolution from APAM to HMAPAM-D (4.5:0.5, optimal) and HMAPAM-E (4:1, excessive hydrophobic modification).

SEM images of APAM, HMAPAM-D, and HMAPAM-E are presented in Figure 8. At relatively low magnification, APAM exhibited discrete particulate morphology with limited aggregation, whereas HMAPAM-D displayed a comparatively loose and interconnected structure. In contrast, HMAPAM-E tended to form more compact agglomerated domains with reduced apparent porosity. These morphological differences qualitatively suggest that hydrophobic modification altered the intermolecular association behavior of the polymer chains.

At higher magnification, APAM particles exhibited relatively smooth surfaces, whereas HMAPAM-D showed roughened surfaces accompanied by wrinkles and lamellar-like features, indicating enhanced structural heterogeneity after hydrophobic modification. Such structural features may facilitate intermolecular interactions and improve the accessibility of adsorption sites during flocculation. In comparison, HMAPAM-E exhibited densely packed regions together with localized collapse-like structures, which may be associated with excessive hydrophobic self-association and restricted chain extension at high LA dosage.

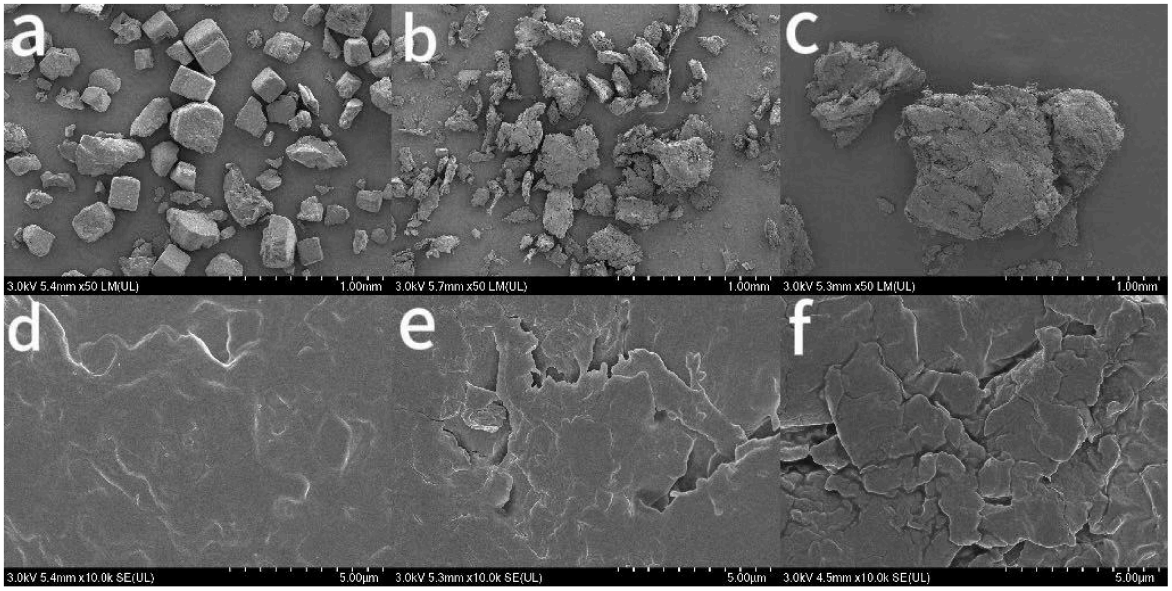


Figure 8. SEM micrographs of pristine APAM (**a**,**d**), HMAPAM-D (**b**,**e**), and HMAPAM-E (**c**,**f**) at magnifications of 50× (**a**–**c**) and 10,000× (**d**–**f**).

Overall, the SEM observations qualitatively support the conclusion that moderate hydrophobic modification promotes a relatively extended polymer microstructure, whereas excessive hydrophobic incorporation tends to induce compact aggregation behavior. It should be noted that SEM observations in this study were primarily used for qualitative morphology analysis rather than quantitative structural characterization.

3.2. Floc Structure Analysis

SEM images of raw coal and coal flocculated with APAM, HMAPAM-D (4.5:0.5), and HMAPAM-E (4:1) are shown in Figure 9.

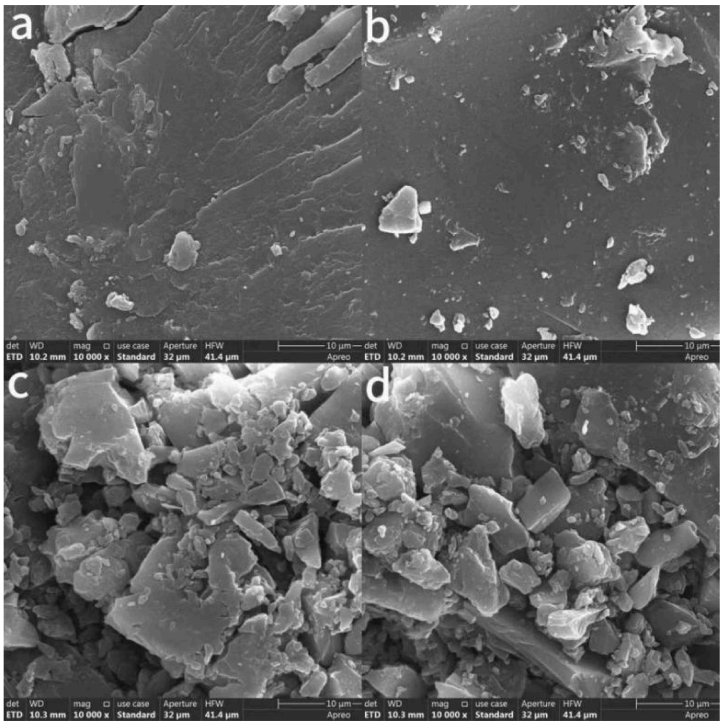


Figure 9. SEM micrographs (10,000×) of coal particle surfaces: (**a**) raw coal; (**b**) coal + APAM; (**c**) coal + HMAPAM-D (4.5:0.5); (**d**) coal + HMAPAM-E (4:1).

SEM images of raw coal particles and flocculated samples are presented in Figure 9. Raw coal particles exhibited relatively smooth surfaces with no observable polymer attachment, indicating the absence of interparticle bridging structures. After treatment with APAM, only sporadic and heterogeneous polymer adhesion was observed on the particle surfaces, suggesting relatively limited bridging interaction and non-uniform floc formation.

In contrast, HMAPAM-D formed a comparatively uniform flocculent coating accompanied by a continuous three-dimensional interconnected network structure between coal particles. This morphology indicates enhanced adsorption bridging and intermolecular association capability after moderate hydrophobic modification, which is favorable for the formation of structurally integrated flocs. The relatively open and interconnected floc structure is expected to facilitate particle aggregation while maintaining sufficient network permeability for water migration during dewatering. However, HMAPAM-E exhibited localized aggregation regions together with irregular polymer coverage and excessive particle encapsulation. Excessive hydrophobic association at high LA dosage may promote partial polymer chain collapse and localized self-aggregation, thereby reducing effective chain extension and adsorption accessibility. Consequently, although particle aggregation still occurred, the resulting floc structure became less uniform and more compact, which may adversely affect floc stability and permeability.

The evolution from heterogeneous surface attachment in APAM to a relatively uniform interconnected structure in HMAPAM-D, followed by localized aggregation behavior in HMAPAM-E, is consistent with the subsequently observed variations in settling and pressure filtration performance.

3.3. Settling Performance

Figure 10 presents the settling performance of APAM and HMAPAM (A–E) as a function of flocculant dosage, including interface settling behavior (Figure 10a), compression layer height (Figure 10b), and supernatant turbidity (Figure 10c). All flocculants rapidly formed distinct solid–liquid interfaces at relatively low dosages, indicating efficient particle aggregation after polymer addition. Compared with unmodified APAM, the HMAPAM series exhibited consistently enhanced settling behavior over the investigated dosage range. Among them, HMAPAM-D achieved the highest interface settling velocity of 0.817 cm/s at 9 mg/L, representing an increase of 50.2% relative to APAM.

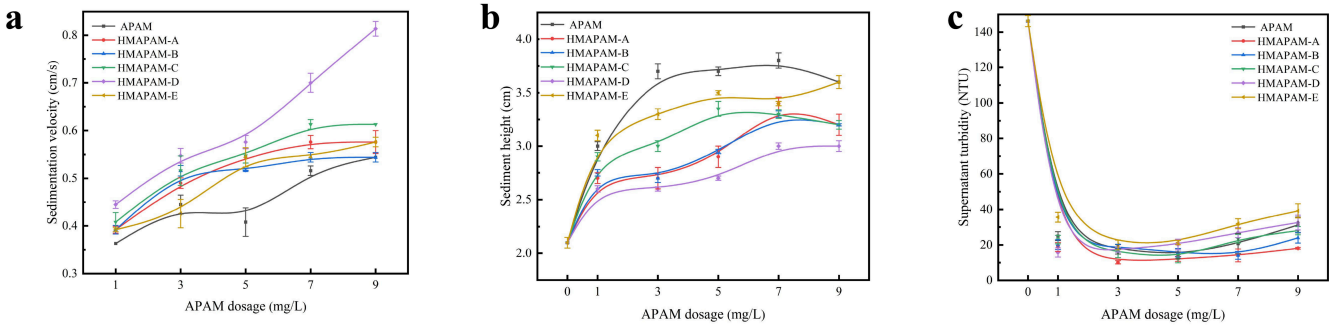


Figure 10. Effect of flocculant dosage on the settling performance of unmodified APAM and HMAPAM (A–E) series: (**a**) settling velocity; (**b**) sediment height after 20 min settling; and (**c**) supernatant turbidity.

The improved settling behavior after hydrophobic modification can be attributed to enhanced intermolecular hydrophobic association between polymer chains, which promotes adsorption bridging and facilitates the formation of larger and structurally integrated flocs. Moderate incorporation of hydrophobic lauryl side chains is conducive to polymer chain extension in solution, thereby increasing effective collision and capture probabili-

ties between coal particles. Similar enhancement mechanisms induced by hydrophobic association have also been reported in previous studies on amphiphilic polyacrylamide flocculants [34].

The sediment heights of HMAPAM-treated samples were generally lower and less dosage-dependent than those obtained with APAM. HMAPAM-D maintained relatively stable sediment heights within 2.6–3.0 cm across the investigated dosage range, suggesting the formation of structurally stable flocs with balanced compactness and network permeability. Such interconnected floc structures are beneficial for maintaining internal drainage pathways while preventing excessive collapse of the sediment bed during consolidation. In contrast, APAM-generated flocs exhibited comparatively weaker structural integrity, resulting in higher sediment heights after settling.

Supernatant turbidity decreased sharply at low dosages for all flocculants, confirming efficient fine-particle capture during the initial flocculation stage. However, a slight turbidity increase was observed at higher dosages for the highly hydrophobically modified samples, particularly HMAPAM-E. This behavior may be associated with excessive hydrophobic self-association and localized polymer aggregation under overdosing conditions, which can partially reduce effective chain extension and steric accessibility for adsorption bridging. As a result, the floc structure becomes less uniform despite continued particle aggregation, leading to reduced settling efficiency and partial deterioration of clarification performance.

Although increasing hydrophobic modification generally improved settling performance, excessive incorporation of hydrophobic groups was not always beneficial. In HMAPAM-E, excessive intramolecular association likely restricted polymer chain dispersion in solution and weakened effective bridging interactions between particles. Consequently, HMAPAM-D (APAM/LA = 4.5:0.5) achieved the optimal balance between hydrophobic association, chain extension, and floc structural stability under the investigated conditions.

Similar enhancement in settling behavior induced by hydrophobic association has also been reported for amphiphilic polyacrylamide flocculants used in fine particle separation [35], indicating that moderate hydrophobic modification can effectively improve adsorption bridging and floc structural stability.

3.4. Pressure Filtration Dewatering Performance

Figure 11 presents the pressure filtration dewatering performance of APAM and HMAPAM (A–E) as a function of flocculant dosage, including filter cake moisture (Figure 11a), cake formation time (Figure 11b), and filtrate turbidity (Figure 11c).

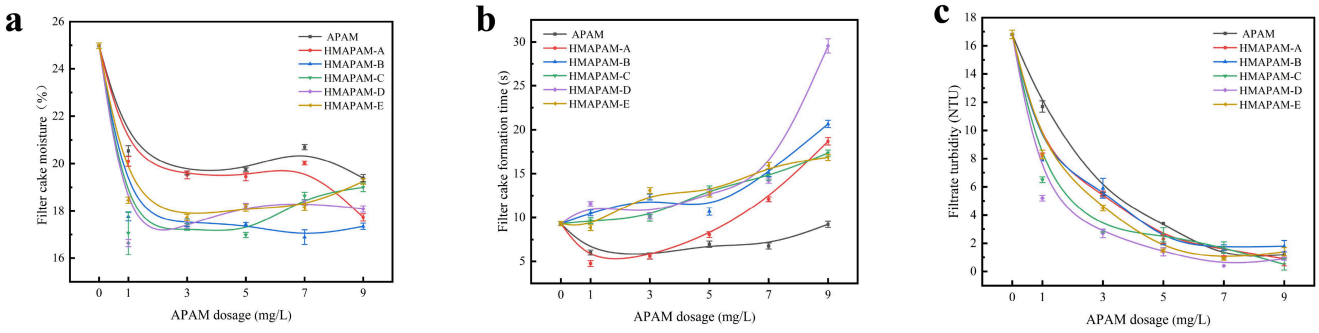


Figure 11. Effect of flocculant dosage on the pressure filtration dewatering performance of unmodified APAM and HMAPAM (A–E) series at 0.6 MPa: (**a**) filter cake moisture; (**b**) filter cake formation time; and (**c**) filtrate turbidity.

Compared with APAM, the hydrophobically modified flocculants achieved significantly lower filter cake moisture contents at substantially reduced dosages. APAM exhibited a minimum cake moisture of 19.39% at 9 mg/L, whereas HMAPAM-D achieved the lowest moisture content of 16.64% at only 1 mg/L. Similarly, HMAPAM-C and HMAPAM-B reached minimum moisture contents of 16.98% and 16.89% at 5 mg/L and 7 mg/L, respectively. These results demonstrate that moderate hydrophobic modification can markedly enhance dewatering efficiency while reducing reagent consumption. The reduction in cake moisture after hydrophobic modification is attributed to multiple synergistic effects. First, the incorporation of hydrophobic lauryl side chains enhances hydrophobic interactions between the polymer and coal particle surfaces, thereby weakening hydration interactions associated with oxygen-containing functional groups. Second, moderate intermolecular hydrophobic association promotes the formation of interconnected floc structures with improved structural integrity and internal drainage pathways, facilitating water migration during pressure filtration. In addition, partial shielding of hydrophilic functional groups may reduce capillary and adsorbed water retention within the filter cake structure.

However, excessive hydrophobic modification was not beneficial for further dewatering improvement. When the APAM/LA ratio increased to 4:1 (HMAPAM-E), the filter cake moisture increased again despite continued particle aggregation. Excessive hydrophobic association may induce localized polymer self-aggregation and partial chain collapse, resulting in denser floc structures and reduced cake permeability. Such compact structures can restrict internal water transport and hinder efficient drainage during filtration. The cake formation time results further support this mechanism. At relatively low dosages, moderate hydrophobic modification shortened cake formation time owing to the formation of relatively permeable floc networks with lower filtration resistance. HMAPAM-A achieved the shortest cake formation time of 4.74 s at 1 mg/L. However, with increasing dosage, the cake formation time of highly modified systems increased sharply, particularly for HMAPAM-D, which reached 29.56 s at 9 mg/L. This behavior suggests that excessive polymer addition promotes overdevelopment of the floc network and increases specific cake resistance, thereby slowing filtrate passage despite the relatively low final cake moisture.

Therefore, low filter cake moisture and rapid filtration are not necessarily achieved simultaneously. Moderate hydrophobic modification at an appropriate dosage improves both floc structural integrity and drainage capability, whereas excessive dosage or excessive hydrophobic association may lead to dense cake structures with restricted permeability and prolonged filtration time. Filtrate turbidity decreased progressively with increasing dosage for all flocculants, confirming improved solid–liquid separation after polymer addition. Among the investigated samples, HMAPAM-D achieved the lowest filtrate turbidity of 0.4 NTU at 7 mg/L, indicating efficient fine-particle capture and stable floc formation. However, the clarification performance slightly deteriorated for HMAPAM-E at high dosage, which may be related to localized aggregation and reduced adsorption accessibility caused by excessive hydrophobic self-association.

Previous studies have shown that hydrophobically modified PAM flocculants can reduce filter cake moisture to approximately 17–22% depending on coal type and operating conditions [36]. In the present study, HMAPAM-D achieved a cake moisture of 16.64% at a relatively low dosage, demonstrating competitive dewatering performance.

4. Conclusions

HMAPAM flocculants were successfully synthesized through free-radical graft copolymerization of lauryl acrylate (LA) onto APAM (Mw = 1.2×10^7). FTIR, ^{1}H NMR, and XPS analyses confirmed the progressive incorporation of hydrophobic alkyl side chains and the gradual reduction in surface polarity with increasing LA dosage. Moderate hydrophobic

modification significantly enhanced both settling and pressure filtration dewatering performance. Among the investigated samples, HMAPAM-D (APAM/LA = 4.5:0.5) exhibited the optimal performance, achieving a maximum interface settling velocity of 0.817 cm/s at 9 mg/L, representing a 50.2% increase relative to APAM, while reducing filter cake moisture to 16.64%. The improved dewatering behavior is attributed to the synergistic effect of hydrophobic association and adsorption bridging. Moderate incorporation of hydrophobic side chains promoted intermolecular association and polymer chain extension, facilitating the formation of interconnected floc structures with improved structural stability and internal drainage capability. Meanwhile, hydrophobic interactions between alkyl chains and coal particle surfaces, together with hydrogen bonding between amide groups and oxygen-containing functional groups on coal surfaces, enhanced particle capture and floc formation.

However, excessive hydrophobic modification intensified intramolecular self-association and restricted effective chain extension, leading to localized aggregation, increased filtration resistance, and deterioration of dewatering performance. Therefore, an appropriate balance between hydrophobic association and polymer chain accessibility is essential for achieving efficient flocculation–dewatering performance in low-rank coal slurry systems.

Author Contributions: Conceptualization, Q.Z., H.Z. and K.N.; Methodology, Q.Z., H.X., J.D. and W.L.; Software, X.D.; Validation, X.D.; Formal analysis, L.G.; Investigation, R.Z. and H.Z.; Resources, L.G. and W.L.; Data curation, R.Z. and K.N.; Writing—original draft, Q.Z.; Writing—review & editing, Q.Z. and K.N.; Supervision, H.X. and H.Z.; Project administration, J.D.; Funding acquisition, J.D. and W.L. All authors have read and agreed to the published version of the manuscript.

Funding: This research was funded by the National Key R&D Program of China (No. 2024YFC2909800), the Fundamental Research Funds for the Central Universities (No. 2025ZKPYHH03).

Data Availability Statement: The original contributions presented in this study are included in the article. Further inquiries can be directed to the corresponding authors.

Conflicts of Interest: Author Leilei Gao was employed by the Datang Tongzhou Technology Co., Ltd., Beijing 100000, China. The remaining authors declare that the research was conducted in the absence of any commercial or financial relationships that could be construed as a potential conflict of interest.

References

1. Liu, L.; Zhuo, Q.; Xu, H.; Wang, D. A Measurement Method for the Pore Structure of Coal Slime Filter Cake. *Processes* **2022**, *11*, 102. [CrossRef]
2. Ren, B.; Lv, K.; Min, F.; Chen, J.; Liu, C. A New Insight into the Adsorption Behavior of NPAM on Kaolinite/Water Interface: Experimental and Theoretical Approach. *Fuel* **2021**, *303*, 121299. [CrossRef]
3. Samoshina, Y.; Diaz, A.; Becker, Y.; Nylander, T.; Lindman, B. Adsorption of Cationic, Anionic and Hydrophobically Modified Polyacrylamides on Silica Surfaces. *Colloids Surf. Physicochem. Eng. Asp.* **2003**, *231*, 195–205. [CrossRef]
4. Zou, W.; Gong, L.; Huang, J.; Zhang, Z.; Sun, C.; Zeng, H. Adsorption of Hydrophobically Modified Polyacrylamide P(AM-NaAA-C16DMAAC) on Model Coal and Clay Surfaces and the Effect on Selective Flocculation of Fine Coal. *Miner. Eng.* **2019**, *142*, 105887. [CrossRef]
5. Muratspahić, E.; Brandfellner, L.; Schöffmann, J.; Bismarck, A.; Müller, H.W. Aqueous Solutions of Associating Poly(Acrylamide-Co-Styrene): A Path to Improve Drag Reduction? *Macromolecules* **2022**, *55*, 10479–10490. [CrossRef]
6. Ho, Y.; Norli, I.; Alkarkhi, A.F.; Morad, N. Characterization of Biopolymeric Flocculant (Pectin) and Organic Synthetic Flocculant (PAM): A Comparative Study on Treatment and Optimization in Kaolin Suspension. *Bioresour. Technol.* **2010**, *101*, 1166–1174. [CrossRef]
7. Lee, K.E.; Morad, N.; Poh, B.T.; Teng, T.T. Comparative Study on the Effectiveness of Hydrophobically Modified Cationic Polyacrylamide Groups in the Flocculation of Kaolin. *Desalination* **2011**, *270*, 206–213. [CrossRef]
8. Liu, J.; Liu, H.; He, C.; Xiao, H.; Jin, M.; Yao, H. Correlation between Sewage Sludge Pore Structure Evolution and Water Filtration Performance: Effect of Thermal Hydrolysis with or without Carbonaceous Skeleton-Assisted. *Water Res.* **2025**, *268*, 122578. [CrossRef]

9. Chen, R.; Dong, X.; Feng, Z.; Fan, Y.; Ma, X. Effect of Froth on the Interaction Between Coal Particles and Cake Structures in the Dewatering Process of Clean Coal. *Processes* **2024**, *12*, 2738. [CrossRef]
10. Qi, S.; Song, Y.; Zhou, S.; Zhang, J.; Peng, Y. Effect of Ion Type and Molecular Weight of Polyacrylamide on Dewatering Performance of Flotation Clean Coal. *Physicochem. Probl. Miner. Process.* **2025**, *61*, 204126. [CrossRef]
11. Hu, P.; Liang, L.; Xie, G.; Zhou, S.; Peng, Y. Effect of Slurry Conditioning on Flocculant-Aided Filtration of Coal Tailings Studied by Low-Field Nuclear Magnetic Resonance and X-Ray Micro-Tomography. *Int. J. Min. Sci. Technol.* **2020**, *30*, 859–864. [CrossRef]
12. Yang, A.; Liao, Y.; An, M.; Cao, Y.; Yang, Z.; Ren, H.; Su, H.; Zou, Q.; Chen, L. Effect of Surfactant and Flocculant on Low-Rank Coal Slime Filtration: From Filter Cake Characteristics Point of View. *Fuel* **2022**, *327*, 125136. [CrossRef]
13. Xu, S.; Shi, J.; Sun, H.; Deng, J.; He, Z.; Ye, Z.; Wang, Y. Effects of a New Synthetic Fe-PAM Flocculants on Filtration and Consolidation of Bentonite Slurry. *Constr. Build. Mater.* **2024**, *439*, 137331. [CrossRef]
14. Bratskaya, S.; Avramenko, V.; Schwarz, S.; Philippova, I. Enhanced Flocculation of Oil-in-Water Emulsions by Hydrophobically Modified Chitosan Derivatives. *Colloids Surf. Physicochem. Eng. Asp.* **2006**, *275*, 168–176. [CrossRef]
15. Lai, Q.; Liao, Y.; Liu, Z. Enhanced Low-Rank Coal Slime Dewatering by Adjustment of Channel Wall Structure and Surface Wettability. *Sep. Purif. Technol.* **2020**, *248*, 116970. [CrossRef]
16. Ping, A.; Peng, Y.; Xie, G.; Wang, M.; Xia, W. Enhancement of Dewatering Performance of Vitrinite-Rich and Inertinite-Rich Coals by Surfactants: Experiment and Simulation. *Fuel* **2022**, *318*, 123571. [CrossRef]
17. Wang, D.; Wang, D.; Zhang, H.; Bollneni, L.; Bayarsaikhan, B.; Liu, Q. Examining the Effect of Conditioning Sequence of Polymer Flocculants and Coagulants on Sedimentation and Filtration of Oil Sands Tailings. *Miner. Eng.* **2025**, *228*, 109324. [CrossRef]
18. Shaban, M.; Ramazani S.A, A.; Ahadian, M.; Tamsilian, Y.; Weber, A. Facile Synthesis of Cauliflower-like Hydrophobically Modified Polyacrylamide Nanospheres by Aerosol-Photopolymerization. *Eur. Polym. J.* **2016**, *83*, 323–336. [CrossRef]
19. Xu, G.; Liu, L.; Geng, D.; Shao, H.; Wang, H.; Tao, D.; Liu, Z.; Bilal, M. Flocculation and Filtration Performance of Coal Slime Water: Role of Flocculant Molecular Weight and Coagulants. *Int. J. Coal Prep. Util.* **2025**, *46*, 1160–1172. [CrossRef]
20. Liu, H.; Yang, X.; Zhang, Y.; Zhu, H.; Yao, J. Flocculation Characteristics of Polyacrylamide Grafted Cellulose from Phyllostachys Heterocycla: An Efficient and Eco-Friendly Flocculant. *Water Res.* **2014**, *59*, 165–171. [CrossRef]
21. Ren, H.; Li, Y.; Zhang, S.; Wang, J.; Luan, Z. Flocculation of Kaolin Suspension with the Adsorption of N,N-Disubstituted Hydrophobically Modified Polyacrylamide. *Colloids Surf. Physicochem. Eng. Asp.* **2008**, *317*, 388–393. [CrossRef]
22. Wang, L.; Min, F.; Chen, J.; Zhang, L.; Liu, L.; Liu, C. Flocculation Performance and Mechanism of P (DMDAAC-AM) on Clay Mineral Layer: Insights from DFT Calculation and Experiment. *Appl. Surf. Sci.* **2023**, *607*, 155089. [CrossRef]
23. Yang, J.; Wang, X.H.; Parekh, B.K. Improved Techniques for Hyperbaric Filtration of Fine Coal Slurry. *Int. J. Coal Prep. Util.* **2010**, *30*, 32–43. [CrossRef]
24. Ren, B.; Xu, M.; Huang, X.; Zhu, J.; Liu, C.; Min, F. Influence of Polyacrylamide-Based Flocculant Dosing Sequence on the Flocculation Bridging Mechanism of Kaolinite: Experimental and MD Simulation Insights. *Surf. Interfaces* **2026**, *83*, 108528. [CrossRef]
25. Hu, S.; Ren, B.; Min, F.; Xu, M.; Huang, X.; Zhu, J. Low-Pressure UV-Initiated Synthesis of Hydrophobic Modified Flocculant P(AM-MAPTAC-TEMAC6) and Investigation of Its Flocculation-Dewatering Performance. *Mater. Today Commun.* **2025**, *49*, 113881. [CrossRef]
26. Zhuo, Q.; Wang, D.; Xu, H.; Liu, W.; Gao, L. Pore Structure and Permeability of Filter Cake in Coal Slurry Filtration. *Int. J. Coal Prep. Util.* **2022**, *42*, 155–170. [CrossRef]
27. Min, F.; Chen, J.; Peng, C.; Chen, C. Promotion of Coal Slime Water Sedimentation and Filtration via Hydrophobic Coagulation. *Int. J. Coal Prep. Util.* **2021**, *41*, 815–829. [CrossRef]
28. Yahaya, G.; Ahdab, A.; Ali, S.; Abu-Sharkh, B.; Hamad, E. Solution Behavior of Hydrophobically Associating Water-Soluble Block Copolymers of Acrylamide and N-Benzylacrylamide. *Polymer* **2001**, *42*, 3363–3372. [CrossRef]
29. Li, P.; Shen, Y.; Yang, X. Solution Properties and Flocculation of Hydrophobically Associating Cationic Fluorinated Polyacrylamide. *Polym. Bull.* **2011**, *67*, 961–973. [CrossRef]
30. Guo, W.; Zhang, H.; Ma, Z. Study of Synthesis and Flocculation Properties of New Modified Hydrophobic Organic Polymer P(AM-DM-DMC12). *Int. J. Polym. Sci.* **2019**, *2019*, 1–9. [CrossRef]
31. Yang, Y.; Liu, L.; Zhao, H.; Han, L.; Hu, B.; Yu, W.; Zhu, Z.; Li, Z. Study on the Mechanism of the Effect of Plasma Modified APAM on the Sedimentation of Kaolinite Particles. *Miner. Eng.* **2025**, *233*, 109592. [CrossRef]
32. *GB/T 477–2008*; Method for Size Analysis of Coal. Standardization Administration of the People's Republic of China: Beijing, China, 2008.
33. *GB/T 212–2008*; Proximate Analysis of Coal. Standardization Administration of the People's Republic of China: Beijing, China, 2008.
34. Feng, X.; Wan, J.; Deng, J.; Yue, X.; Yang, Y.; He, Z.; Fang, X.; Chen, T.; Li, S.; Lu, J.; et al. Study on the Regulation of Sludge Dewatering by Hydrophobically Associating Cationic Polyacrylamide Coupled with Framework Materials. *J. Water Process Eng.* **2022**, *45*, 102502. [CrossRef]

35. Liu, R.; Yuan, J.; Huang, L.; Yu, S.; Zhao, Y.; Duan, C.; Jiang, H. Synergistic Enhancement of Coal Slurry Water Sedimentation and Dehydration Process Using PDMDAAC/PAM. *J. Clean. Prod.* **2024**, *434*, 140160. [CrossRef]
36. Shi, Z.; Liu, L. Synergistic Mechanism of CTAB and Nonionic Polyacrylamide on Pore Structure of Kaolinite Filter Cake. *Sep. Purif. Technol.* **2023**, *324*, 124575. [CrossRef]

Disclaimer/Publisher's Note: The statements, opinions and data contained in all publications are solely those of the individual author(s) and contributor(s) and not of MDPI and/or the editor(s). MDPI and/or the editor(s) disclaim responsibility for any injury to people or property resulting from any ideas, methods, instructions or products referred to in the content.